Tool positioning error (TPE) characterisation in milling

Yann Landon, Stéphane Segonds, Pierre Lascoumes, Pierre Lagarrigue

Tool positioning error (TPE) characterisation in milling

Yann Landon *, Stéphane Segonds, Pierre Lascoumes, Pierre Lagarrigue

Laboratoire de Génie Mécanique de Toulouse, Bât.3R1, Université Paul Sabatier, 118 Rte de Narbonne, 31062 Toulouse Cedex 4, France

Received 29 October 2002; received in revised form 13 November 2003; accepted 1 December 2003

Abstract

Where the geometrical features so permit, the {workpiece–work-holding fixture} assembly is generally considered to be infinitely rigid. The {tool–tool-holder–spindle} assembly and the machine axes are then deformed under the action of the cutting forces. This deformation leads to a positioning error of the tool in relation to the theoretical position. With the aim of taking this positioning error into account, the inaccuracies obtained during end milling and side milling were experimentally modelled from the cutting conditions used for a given machine/mill/material triplet (TriM). Our "Virtual Worker" then used these models to predict machining errors according to the type of machining and to compensate for them.

Keywords: Milling errors modelling; Tool positioning error (TPE); Virtual Worker

1. Introduction

In the current industrial context with the permanent quest for quality, it is essential to take into account errors that occur when manufacturing the workpieces that make up mechanical systems. This involves knowledge of phenomena prejudicial to quality and their influence on the conformance of workpieces to functional specifications. Taking milling errors into account, especially the tool positioning error (TPE, often reduced to tool flexion only), involves two stages:

- Quantification of the error: milling inaccuracy is evaluated in relation to the case of milling studied (cutting conditions, workpiece material, tool, machine, etc.);
- Compensation of the error during milling: compensation involves either determining the milling parameters that offer least and most acceptable inaccuracy with respect to the associated tolerance interval, or modification of milling trajectories (or even positioning of the tool) so that the error may be compensated for, either partly or in full.

For the quantification phase, the general method described in the literature is as follows:

- Construction of a model of forces: the cutting forces are expressed in relation to the milled material, the tool (geometry and material) and the cutting conditions;
- Construction of a deformation model: only tool flexion is considered; it is determined from the previously calculated force and the tool's geometrical and mechanical characteristics.

Basically, two types of mechanistic force model are developed in the literature with detailed variations, depending on the author. Some methods merely seek to express the resultant of the workpiece's action on the tool, as projected in different directions. Generally, for the first type, we have:

$$F_c = K \cdot h \cdot a_p \quad (1)$$

In this case, the specific cutting pressure K can be determined by adapting standard coefficients or through experience. The calculation for the chip thickness h may also vary from one author to another. Adolfsson and Ståhl [1] seek to take into account variation in the radial position of each tooth, wear in the teeth and non-coincidence between the tool centre and

* Corresponding author. Tel.: +33-5-61-55-81-76; fax: +33-5-61-55-81-78.

E-mail address: landon@cict.fr (Y. Landon).

. doi:10.1016/j.ijmachtools.2003.12.001

Nomenclature

β	angle of rotation in the XY plane between the tool/workpiece point of contact on a helix and end of the corresponding tooth
δ	flexion at tool tip (mm)
$\delta(z)$	flexion on dimension z of tool tip (mm)
θ	angle of rotation in the XY plane between the tool/workpiece point of contact on a helix and the end of the next tooth
λ	tool helix angle
a_e	radial engagement (mm)
a_p	axial engagement (mm)
da	infinitesimal axial engagement (mm)
dF_t	infinitesimal tangential force of workpiece on the tool (N)
$dpof_i$	TPE for TriM "i" in flank milling (mm)
$dpof_{i\_0}$	TPE for TriM "i" in flank milling on dimension $Z = 0$ (mm)
$dpof_{i\_30}$	TPE for TriM "i" in flank milling on dimension $Z = 30$ (mm)
$dpof_{i\_dep}$	TPE for TriM "i" in flank milling on the depression (mm)
$dpof_{i\_T}$	TPE for TriM "i" in flank milling at the tool tip (mm)
$dpof_{i\_H}$	TPE for TriM "i" in flank milling tool-holder side (mm)
$dpor_i$	TPE for TriM "i" in end milling (mm)
dS	infinitesimal element of the cutting edge length (mm)
D	tool diameter
E	tool elasticity modulus (MPa)
f_z	feed rate per tooth (mm/tooth)
F, F_c	mechanical action of the workpiece on the tool resisting cutting force (N)
h, h_m	mean chip thickness (mm)
I	moment of inertia of the tool (mm^4)
K	specific cutting pressure (MPa)
K_t	tangential specific cutting pressure (MPa)
K_{tc}	tangential specific cutting pressure on the cutting face (MPa)
K_{te}	tangential specific cutting pressure on the cutting edge (N/mm)
L, L_s	free tool length (mm)
L_1	length of tool-holder (mm)
R	tool radius (mm)
TDB	tool data block
TPE	tool positioning error
TriM	machine/mill/material triplet
V_f	feed speed (mm/min)
z_F	axial position of the point of application of the workpiece/tool mechanical action (mm)
z_M	size along Z of the tool/workpiece point of contact or position on Z of the depression (mm)

the centre of rotation. These geometrical variations in the cut are expressed for each tooth in calculating the chip thickness. Kim and Ehmann [2] express cutting force in relation to the angular position of the tooth (i.e. time) and thus use a chip thickness that varies over time. Charbonnaud et al. [3] calculate the mean chip thickness to express a mean cutting force.

The second type of cutting force model often employed is based on breaking up the cutting edge into infinitesimal elements on which infinitesimal forces are expressed. The following formulation is commonly found [4–7], derived from the work of Kline and DeVor [8–10]:

$$dF_t = K_t \cdot h \cdot da \tag{2}$$

Altintas and Lee [11] add the influence of friction on the cutting edge to this model:

$$dF_t = K_{te} \cdot dS + K_{tc} \cdot h \cdot da \tag{3}$$

Different cutting force prediction models are therefore proposed in the literature. Each of these models is built from a precise case with a geometrical study of the milling operation under consideration being conducted before implementation of the model. It can also be noted that there is a real problem of reproducibility

of the predictions due to the amount of influential parameters. Thus, there is a lack of precision in the prediction of cutting forces (up to 20% or 25% of maximum error according to the authors), that introduces a significant error in the prediction of tool deflection.

The link between cutting force and tool flexion has also been covered by a number of workers, leading to different models. But all these are based on assimilating the tool with a deformable beam embedded in the tool-holder, which is considered to be rigid (Fig. 1).

Wang [12] provides with the most simplistic model (Fig. 1(a)). This model assumes that the mechanical action of the workpiece on the tool can be assimilated with a limited effort applied at the tool tip:

$$\delta = \frac{F \cdot L^3}{3 \cdot E \cdot I} \tag{4}$$

where L is the tool length, E its elasticity modulus and I is the moment of inertia of the tool.

DeVor et al. [13] propose a more advanced model in which the point of application of the force is not automatically set at the tool tip:

$$\delta = \frac{F \cdot (2 \cdot L + z_F) \cdot (L - z_F)^2}{6 \cdot E \cdot I} \tag{5}$$

where δ is the flexion at tool tip and z_F is the axial position of the point of application of the force in relation to the tool tip. The tool flexion $\delta(z)$ can also be calculated at any point at distance z from the tool tip [8], as shown Fig. 1(b):

$$\delta(z) = \frac{F}{2 \cdot E \cdot R^4} \times \left[\langle z_F - z \rangle^3 - (L - z)^3 + 3 \cdot (L - z)^2 \cdot (L - z_F) \right] \tag{6}$$

where $\langle z_F - z \rangle^3$ is a singular function on z and R the tool radius.

Lim et al. [14] develop an expression for flexion that takes the special shape of the tools into account (teeth and helix), as also possible deformation of the tool-holder:

$$\delta(z) = \frac{F}{k(z)} \tag{7}$$

where $k(z)$ is a complex function of z, z_F, L and L_1 the tool post length.

Thus, these models of tool flexion depend on the validity of the forces previously calculated and rely on strict assumptions as to the theory of beams. Further, they apply only to special cutting conditions. Again, such models have been validated to the limited scope of the cases actually studied in the said articles, and are thus not suitable in an industrial context.

The characterisation of the tool's behaviour during cutting described in this paper is based on a different approach. Indeed, rather than assuming an ideal context (spindle and tool-holder infinitely rigid, perfect tool geometry, workpiece material in compliance with specifications, etc.), a global approach is adopted: the aim of this work is to characterise not the tool flexion (deformation of the tool) alone, but TPE due to deformation of the {tool–tool-holder–spindle} assembly. This deformation lead to an offset between the active part of the tool and its theoretical position in relation to the workpiece. This results in a positional inaccuracy of the milled surface in relation to its nominal position. The particularity of the method, compared with the current state-of-the-art, is that the cutting forces are not modelled; the TPE is directly linked to the cutting conditions.

The positioning error of the tool during cutting depends on a number of factors that mainly include the machine and tool used, the workpiece material, the milling operation performed and the cutting conditions applied. Considering that only the {tool–tool-holder–spindle} assembly deform, the behaviour of the machine/mill/material triplet (TriM) was characterised for different milling operations. Cases of end milling and side milling, using different TriMs, were studied; the behaviour of the TriMs in all these instances were modelled. The models obtained were brought together in data blocks specific to the tool and the machine used. Subsequently, the creation of other tool data blocks required other tests. For this purpose, a master workpiece that brought together all characteristic milling operations was produced. Milling this workpiece on a machine with a new tool, and measuring inaccuracies, meant that the associated data block could be filled in. The "Virtual Worker" then uses the tool data blocks for the machine it is associated with, in order to predict and compensate for TPEs coming into play during manufacturing (Fig. 2).

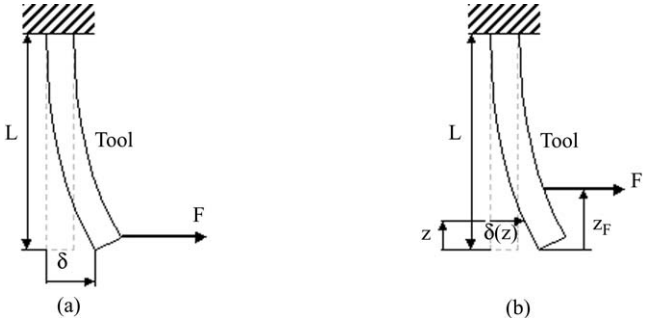

Fig. 1. Base for existing tool flexion models.

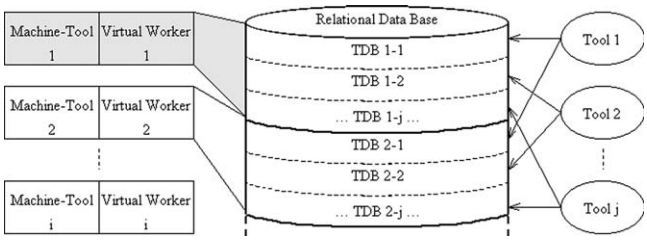

Fig. 2. Architecture for the database bringing TDBs together.

2. Experimental set-up and milling test conditions

To determine the relations between milling errors and the cutting parameters used for the different milling operations, several milling tests were conducted with a first TriM.

The machine used was a horizontal spindle 4-axis machining centre. The kinematics and control for this machine were first tested and corrected [15], together with thermal expansion effects of the spindle [16], in order to eliminate any influence on the present study.

The tool was a TiCN coated HSS flat-end cylindrical milling cutter. It was a 16 mm diameter tool, with 3 teeth, an helix angle of 30° and a cutting length of 32 mm.

The workpiece material we characterised was a C40 unalloyed steel (210 HV).

The experimental set-up is shown in Fig. 3. An isostatic work-holder was used to set-up the test workpieces on the table. The clamping was ensured by strop clamps faced to the supports. The milling tests were performed in the direction of the stop in order to avoid a displacement of the workpiece during cutting.

On the test workpieces (Fig. 4), a reference (composed of a plane and a straight line) was milled so as to be able to neglect deformation of the tool on this portion. This reference was then used to construct a measuring datum. Measurement of the surfaces produced was done using a co-ordinate measuring machine.

End milling operation was characterised by performing a series of slot millings with different cutting conditions, that is: feed per tooth f_z (varying from 0.05 to 0.15 mm/tooth) and the axial engagement a_p (ranging from 1 to 12 mm). The free tool length L_s was also taken into account. Note that these tests were performed for end milling in a single pass; for cases with deep slots milled in a number of passes, it is considered

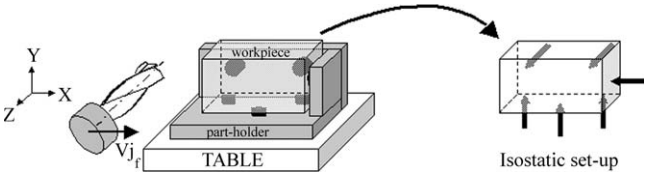

Fig. 3. Experimental set-up.

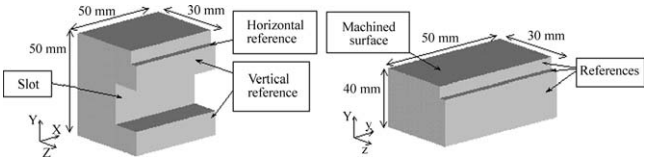

Fig. 4. Test workpieces. (a) End milling test workpiece; (b) side milling test workpiece.

necessary to use contour milling finishing in order to avoid offsets.

Side milling operation was characterised by performing a series of flank milling operations with different cutting conditions, that is: feed per tooth f_z (varying from 0.05 to 0.15 mm/tooth), the radial engagement of the tool a_e (ranging from 0.5 to 5 mm) and the axial engagement a_p (ranging from 10 to 30 mm). Initially, down milling only was undertaken, as this is used in industry for finishing passes. The surface was first cleaned (with the same tool and a radial engagement smaller than 0.1 mm) to guarantee constant tool radial engagement.

Other tests (end millings and side millings) were performed with different TriMs (two machining centres, three HSS tools and two steels) in order to validate the observed behaviour.

3. Experimental results and discussion

Each test workpiece was measured on the CMM in order to quantify the TPE in each case. For each milling operation type (end milling and side milling), the tests showed that measured errors could be linked to cutting conditions (L_s, f_z and a_p in end milling; f_z, a_e and a_p in side milling).

3.1. Case of end milling

The slot position along the Y-axis was measured in relation to the horizontal reference. Firstly, it was noted that the position of a slot along Y was constant (straightness along X), apart from the workpiece entry and exit zones. A profile projector and the CMM were used also to determine that distortion of the shape of the slots milled (squareness in relation to the vertical reference) remained insignificant, compared with the positional inaccuracy. Thus, the TPE for the steady-state condition (initially, entry and exit areas were ignored) was characterised by measuring the inaccuracy in the position of slots along the Y-axis. Measured positional inaccuracies were then linked to the cutting conditions (Fig. 5).

A model was constructed giving the TPE in end milling (noted $dpor_i$ for TriM "i") for a given couple of cutting conditions (a_p and h_m, the mean chip thickness)

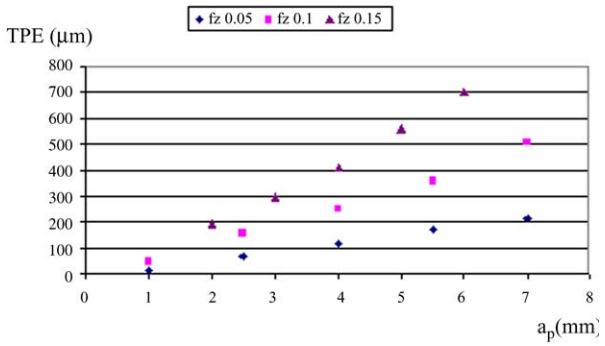

Fig. 5. TPE in end milling related to the cutting conditions used.

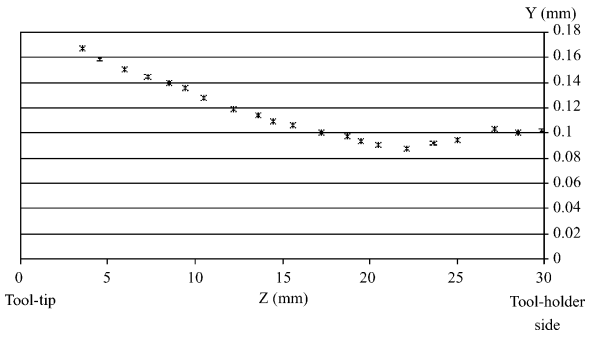

Fig. 7. Shape of the deformed surface.

and a free tool length L_s:

$$\vec{\mathbf{dpor}}_i = K_i(L_s) \cdot \left(a_p^{p_i} \cdot h_m\right)^{q_i} \cdot \vec{y} \tag{8}$$

where K_i is a polynomial of degree 2 on L_s, and p_i and q_i constants for the TriM "i".

This model was validated for all the TriMs studied. Only the coefficients for the polynomial K_i and constants p_i and q_i varied from one TriM to another.

3.2. Case of side milling

In side milling, the deformed surface was examined at a large number of points which were used to "reconstruct" this surface (Fig. 6). This figure does not show the entry surface measurement ($0 < X < 10$ mm) or the exit surface measurement ($40 < X < 50$ mm). The nominal position of the milled surface is shown by the ordinate $Y = 0$.

The mapping obtained highlights four special features of the surfaces produced: firstly, the positioning error (along Y) can be considered constant for a fixed dimension Z, for all X (straightness along X). Further, at attachment side ($Z = 30$ mm in the example), the error was not null. Subsequently, the error diminished slightly as Z diminished: there was a depression on the surfaces, located at about 8 mm from the edge ($Z = 22$ mm) in this example. Finally, the error increased to a maximum value at the far end of the surface ($Z = 0$ mm, tool tip). These four special characteristics existed for each milled workpiece.

Since the error is constant for a fixed dimension Z, the shape of the surface produced can be represented by a cross-section along the plane YZ (Fig. 7). This translates the stationary process for the deformation of the {tool–tool-holder–spindle} assembly at work.

The position along the Z-axis of the depression varied slightly from one workpiece to another. Repetition of the measurements indicates that this depression is real and not due to a measurement error. Indeed, the results obtained on the CMM were identical to those measured on the machine before removal of the workpieces. This characteristic shape is due to the change in cutting forces along the helix during rotation of the tool. When a tooth cuts into the material at the tool tip (Fig. 8), the previous tooth will still be milling on point M. So, there is an angular portion of the tool rotation during which there are two teeth that are milling the workpiece (for $30 < Z < 22$ mm and $8 < Z < 0$ mm for the showed example). During the rest of the rotation, only one tooth is milling (for $22 < Z < 8$ mm for the showed example).

The polar co-ordinates for this point M belonging to the helix (Fig. 9) depend on the tool radius R, the helix

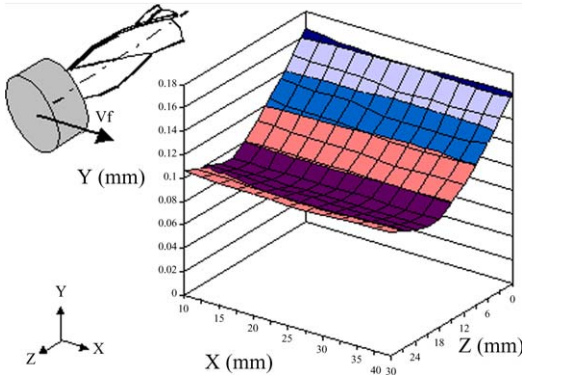

Fig. 6. Reconstruction of the deformed surface of a milled workpiece with $a_p = 30$ mm.

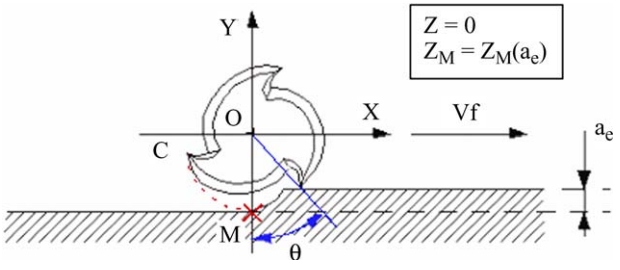

Fig. 8. A tooth cuts into the material at tool tip while point M is still milling at $Z = Z_M$.

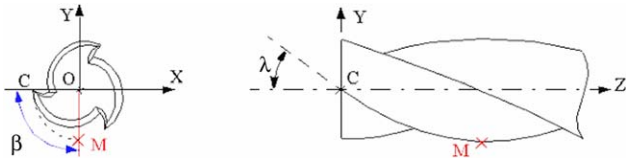

Fig. 9. Reducing the helix to an equation.

angle λ and the angle of rotation β:

$$x_M = R \cdot \cos(\beta) \tag{9}$$

$$y_M = R \cdot \sin(\beta) \tag{10}$$

$$z_M = \frac{R \cdot \beta}{\tan(\lambda)} \tag{11}$$

Using Eq. (11), the dimension along Z for this point M in relation to the angle θ (Fig. 8) and thus for a_e can be calculated as (with n_t the number of teeth of the tool):

$$\beta = \frac{2\pi}{n_t} - \theta = \frac{2\pi}{n_t} - \arccos\left(\frac{R - a_e}{R}\right) \tag{12}$$

$$z_M = \frac{R}{\tan(\lambda)} \cdot \left[\frac{2\pi}{n_t} - \arccos\left(\frac{R - a_e}{R}\right)\right]$$

with $n_t = 3$ in the example (13)

With this equation, for a radial engagement of 1 mm, the dimension along Z for point M is 22 mm. At that moment, there is not yet a tooth engaged at the tool tip ($Z = 0$). The only cutting force is applied at point M with a smaller lever arm than at the tool tip. Immediately after this, the next tooth cuts into the material and a second force is then applied to the tool tip. Thus, deformation of the {tool–tool-holder–spindle} assembly increases. Point M of the tool, which is still milling as it moves towards $Z = 30$, thus moves away and leaves a depression on the surface on dimension $Z = 22$ mm where it was previously.

However, the depression only appears on the workpieces milled with a sufficiently high radial engagement–axial engagement couple. Indeed, it is previously showed that for a radial engagement of 1 mm, the depression appeared at 22 mm from the tool tip. Now, if the axial engagement is less than 22 mm, no depression appears on the workpiece. This explains whether the depression will be present or not on the milled workpieces.

The position of the depression on each workpiece was compared with the results obtained from Eq. (13). The extremely good correlation between the real values obtained and the calculation corroborated the above explanation (Fig. 10). Eq. (13) can thus be taken into account in the modelisation to predict the possible position of a depression on a side milled surface.

To characterise the deformation obtained in side milling in relation to the cutting parameters (f_z, a_e and

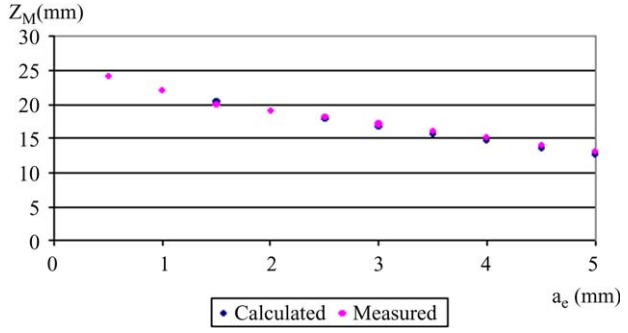

Fig. 10. Comparison between positions for calculated and measured depressions.

a_p), the four special features observed on the surfaces were used. Thus, the real side milled surface will be defined solely on the YZ plane by three values (Fig. 11):

- that for the TPE at the far end of the surface, on the attachment side (noted dpof_{i_H} for TriM "i", H for tool-holder);
- that for the TPE at the tool tip (noted dpof_{i_T} for TriM "i", T for tool-tip); and
- that for the TPE on the depression (noted dpof_{i_dep} for TriM "i", located at $Z = Z_M$).

The models obtained (for all the TriMs studied) were as follows:

$$\text{dpof}_{i\_H}(a_p) = k_{i\_H}(a_p) \cdot (a_e^{p_{i\_H}(a_p)} \cdot h_m)^{q_{i\_H}(a_p)} \tag{14}$$

$$\text{dpof}_{i\_T}(a_p) = k_{i\_T}(a_p) \cdot (a_e^{p_{i\_T}(a_p)} \cdot h_m)^{q_{i\_T}(a_p)} \tag{15}$$

$$\text{dpof}_{i\_dep}(a_p) = k_{i\_dep}(a_p) \cdot (a_e^{p_{i\_dep}(a_p)} \cdot h_m)^{q_{i\_dep}(a_p)} \tag{16}$$

where $k_i(a_p)$, $p_i(a_p)$ and $q_i(a_p)$ are functions of a_p and thus constant for a given axial engagement a_p. The variable h_m represents the mean chip thickness.

Further, it was also observed the following linear law, verified for dpof_{i_H}, dpof_{i_T} and dpof_{i_dep}:

$$\text{dpof}_i(f_z = 0.1) = \frac{\text{dpof}_i(f_z = 0.05) + \text{dpof}_i(f_z = 0.15)}{2} \tag{17}$$

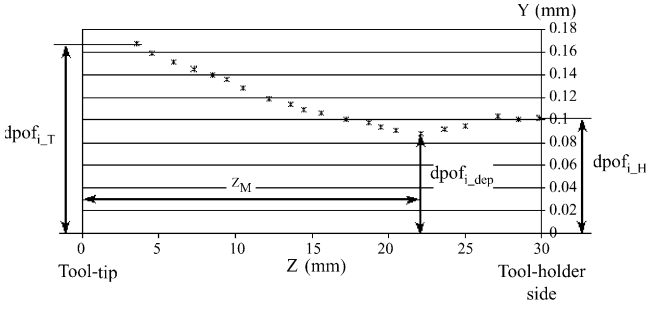

Fig. 11. Illustration of data provided by the models.

This equation can be used to reduce the number of tests to be performed to characterise a TriM in side milling.

Moreover, it was also noted that the shape of the surface obtained in the *YZ* plane can be directly modelled. A single equation then characterises the TPE though the correlation with real conditions is not as good as for the aforementioned models. These models are indeed extremely precise (less than 2% error in relation to the errors measured) and mean that reliable results can be obtained; moreover, these models can be easily readjusted with very few tests for a new TriM. However, the possibility of devising an equation for the surface obtained can be used when it proves necessary.

3.3. Case of up milling

The study conducted above only concerns the case of down milling. Up milling tests were also performed. It was clearly seen from the results obtained that the TPE was near null with up milling (or even negative for large chip volumes). This observation concurred with the result of a study conducted by Lee and Ko [17] that showed that the cutting forces on the tool are not directed in the same way in down milling and in up milling (Fig. 12).

Thus, for up milling, the resultant force is in opposition almost only with the feed speed V_f; the radial deformation of the {tool–tool-holder–spindle} assembly is then practically null. The same phenomenon was noted on the test workpieces.

Up milling would then appear to be a simple and effective solution to the TPE problem. But the influence of the milling direction on the quality of the surface must not be neglected. Indeed, in the engineering industry, finishing milling is always done using down milling to preserve the tools (more rapid deterioration in up milling due to material work hardening) and obtain a better surface finish than can be achieved with up milling. This difference on the workpieces was registered by comparing the surface roughness obtained with down milling and up milling using the same cutting conditions. The results obtained are listed in the table below (Table 1).

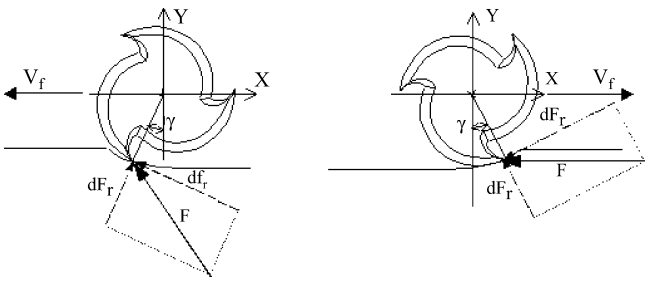

Fig. 12. Direction of cutting forces in down milling (a) and up milling (b).

These results confirm how important the milling direction is when it comes to surface roughness. When high surface quality is not required, up milling can be used to take advantage of the very low TPE. In other cases where good surface quality is required, up milling can be reserved for semi-finishing operations to guarantee a constant machining oversize.

4. Conclusions and future works

The study conducted on end milling and side milling shows there is an opportunity to relate TPEs and the characteristic parameters of the type of milling concerned. It proves the possibility to predict tool deflection without the use of a cutting force model. For each machine/mill/material triplet (TriM) studied, a data block was created, including the set of models characterising its behaviour in end milling and in side milling. Thus, for each future use of one of these TriMs, it will be possible to predict the TPEs that will appear before milling.

The models drawn up are very accurate since no assumption or approximation is made. They derive directly from experiment and thus faithfully represent reality. The models were constructed by interpolation on the measurement results, and the precision of interpolation was generally smaller than the accuracy of measurement. These models have been tested and validated on 3-axis milling applications (3-axis slots and circular contour millings). The results obtained (Table 2) show that the maximum error of prediction is of 9%, widely smaller than those obtained with the use of a cutting force model. Thus, this method is a solution to the problem of tool deflection prediction and is suitable for concrete cases.

The models were validated for several different TriMs and can thus be considered suitable for other cases. But characterisation of behaviour for a new TriM will necessarily involve devising a number of tests whose measurement results will provide with the means to determine variables for models. With the aim of determining these variables rapidly, a master workpiece was developed bringing together character-

Table 1
Comparison of surface roughness in down and up milling

Product $f_z \cdot a_p \cdot a_e$	R_t perpendicular V_f in down milling (μm)	R_t perpendicular V_f in up milling (μm)
0.75	4.17	8.05
4.5	4.40	8.23
11.25	4.50	9.88

Table 2
Application of the developed models on 3-axis millings

3-Axis slots			Circular slot			Circular contour millings		
Predicted TPE (μm)	Measured TPE (μm)	Error (%)	Predicted TPE (μm)	Measured TPE (μm)	Error (%)	Predicted TPE (μm)	Measured TPE (μm)	Error (%)
26.33	28.5	−7.72	258	261	−1.16	104	111	−6.73
36.73	40	−8.17	258	243	+5.81	104	113	−8.65
53.50	56	−4.47	258	254	+1.55	104	109	−4.81
59.79	65	−8.02	258	263	−1.94	92	100	−8.70
63.99	67.5	−5.19	258	268	−3.88	92	95	−3.26
70.59	75	−5.88	258	239	+7.36	92	97	−5.43
76.39	82.5	−7.40	258	250	+3.10	162	168	−3.70
86.13	94	−8.37	258	276	−6.98	162	174	−7.41
93.31	102.5	−8.97	258	269	−4.26	162	171	−5.55

istic milling tasks. The milling and measurement for this workpiece can then be used to fully characterise the TriM concerned.

In order to use this TPE prediction for tool deflection compensation, a computational code was written, named "Virtual Worker". For a planned milling (with an associated TriM), its aim is to refer to the corresponding tool data block (in the data base) to predict the TPEs that will appear and to compensate for them. The compensation procedure used is the modification of tool paths by taking into account the predicted errors (mirror method). The code and compensation procedure are currently tested with application cases.

References

[1] C. Adolfsson, J.E. Ståhl, Cutting force model for multi-toothed cutting processes and force measuring equipment for face milling, International Journal of Machine Tools and Manufacture 35 (1995) 1715–1728.

[2] H.S. Kim, K.F. Ehmann, A cutting force model for face milling operations, International Journal of Machine Tools and Manufacture 33 (1993) 651–673.

[3] P. Charbonnaud, F.J. Carrillo, D. Ladevèze, Monitored robust force control of a milling process, Control Engineering Practice 9 (2001) 1047–1061.

[4] Y.S. Tarng, C.I. Cheng, J.Y. Kao, Modeling of 3-D numerically controlled end milling operations, International Journal of Machine Tools and Manufacture 35 (1995) 939–950.

[5] W.S. Yun, D.W. Cho, Accurate 3-D cutting force prediction using cutting condition independent coefficients in end milling, International Journal of Machine Tools and Manufacture 41 (2001) 463–478.

[6] G.M. Kim, P.J. Cho, C.N. Chu, Cutting force prediction of sculptured surface ball-end milling using Z-map, International Journal of Machine Tools and Manufacture 40 (2000) 277–291.

[7] E.M. Lim, H.Y. Feng, C.H. Menq, Z.H. Lin, The prediction of dimensional error for sculptured surface productions using the ball-end milling process: chip geometry analysis and cutting force prediction, International Journal of Machine Tools and Manufacture 35 (1995) 1149–1169.

[8] W.A. Kline, R.E. DeVor, R. Lindberg, The prediction of cutting forces in end milling with application to cornering cuts, International Journal of Machine Tool Design and Research 22 (1982) 7–22.

[9] W.A. Kline, R.E. DeVor, An improved method for cutting forces in end milling, International Journal of Machine Tool Design and Research 23 (1983) 123–140.

[10] J.W. Sutherland, R.E. DeVor, The effect of runout on cutting geometry and force and surface error prediction in flexible end milling system, Transactions of ASME, Journal of Engineering Industry 108 (1986) 269–279.

[11] Y. Altintas, P. Lee, Mechanics and dynamics of ball end milling, Transactions of ASME, Journal of Manufacturing Science and Engineering 120 (1998) 684–692.

[12] W.P. Wang, Solid modeling for optimizing metal removal of three-dimensional end milling, Journal of Machining Systems 7 (1988) 57–65.

[13] R.E. DeVor, W.A. Kline, W.J. Zdeblick, A mechanistic model for the force system in end milling with application to machining airframe structures, Proceedings of the Eighth NAMRC, 1980, pp. 297–303.

[14] E.M. Lim, H.Y. Feng, C.H. Menq, Z.H. Lin, The prediction of dimensional error for sculptured surface productions using the ball-end milling process: surface generation model and experimental verification, International Journal of Machine Tools and Manufacture 35 (1995) 1171–1185.

[15] Y. Landon, P. Lagarrigue, F. Monies, W. Rubio, Correction of circularity defects on a N.C. machine tool, Proceedings of the Second International Conference of the Euspen, May 27–31, 2001, pp. 848–851.

[16] S. Segonds, P. Lagarrigue, J.M. Redonnet, W. Rubio, Compensation for machining defects due to spindle dilatation, International Journal of Machine Tools and Manufacture 41 (2001) 1439–1454.

[17] S.K. Lee, S.L. Ko, Improvement of the accuracy in the machining of a deep shoulder cut by end milling, Journal of Materials Processing Technology 111 (2001) 244–249.